A Computational Study of the Oxidation of SO2 to SO3 by Gas-Phase Organic Oxidants

ARTICLE *in* THE JOURNAL OF PHYSICAL CHEMISTRY A · JUNE 2011

Impact Factor: 2.69 · DOI: 10.1021/jp203907d · Source: PubMed

4 AUTHORS, INCLUDING:

Joseph Lane
The University of Waikato
43 PUBLICATIONS **638** CITATIONS
SEE PROFILE

Solvejg Jørgensen
University of Copenhagen
42 PUBLICATIONS **588** CITATIONS
SEE PROFILE

Henrik G Kjaergaard
University of Copenhagen
141 PUBLICATIONS **3,822** CITATIONS
SEE PROFILE

THE JOURNAL OF PHYSICAL CHEMISTRY A

ARTICLE

pubs.acs.org/JPCA

A Computational Study of the Oxidation of SO_2 to SO_3 by Gas-Phase Organic Oxidants

Theo Kurtén,[*,†,‡] Joseph R. Lane,[§] Solvejg Jørgensen,[†] and Henrik G. Kjaergaard[*,†]

[†]Department of Chemistry, University of Copenhagen, Universitetsparken 5, 2100 Copenhagen Ø, Denmark

[‡]Department of Physics, University of Helsinki, POB 64, FIN-00014 Helsinki, Finland

[§]Department of Chemistry, University of Waikato, Private Bag 3105, Hamilton 3240, New Zealand

Supporting Information

ABSTRACT: We have studied the oxidation of SO_2 to SO_3 by four peroxyradicals and two carbonyl oxides (Criegee intermediates) using both density functional theory, B3LYP, and explicitly correlated coupled cluster theory, CCSD(T)-F12. All the studied peroxyradicals react very slowly with SO_2 due to energy barriers (activation energies) of around 10 kcal/mol or more. We find that water molecules are not able to catalyze these reactions. The reaction of stabilized Criegee intermediates with SO_2 is predicted to be fast, as the transition states for these oxidation reactions are below the free reactants in energy. The atmospheric relevance of these reactions depends on the lifetimes of the Criegee intermediates, which, at present, is highly uncertain.

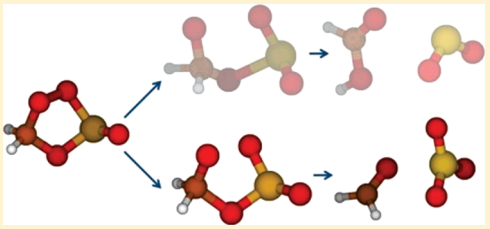

1. INTRODUCTION

The emission of sulfur dioxide is one of the most important mechanisms by which mankind is perturbing the atmosphere. Even though the total mass of anthropogenic sulfur emissions is small compared to that of anthropogenic carbon dioxide emissions, the climate impact of the two pollutants are estimated to be of similar magnitude. According to the emission inventories and radiative forcings from the fourth IPCC assessment report,[1] the short-term radiative forcing associated with a kilogram of sulfur emitted as SO_2 is estimated to be opposite in sign, and 10^4-10^5 times larger in magnitude,[1] than that associated with a kilogram of carbon emitted as CO_2. The reason for this is that SO_2 is oxidized to sulfuric acid (H_2SO_4), the key compound in forming aerosol particles,[2] which, in turn, influence cloud properties and increase the planetary reflectivity (albedo). Sulfuric acid-containing molecular clusters and their possible formation mechanisms have recently been the focus of several experimental and computational studies.[3−6]

The oxidation of SO_2 to H_2SO_4 [also called the S(IV)-to-S(VI) conversion after the oxidation state of the sulfur atom] can occur either in the gas phase or in the aqueous phase of cloud droplets. As a global average, the two pathways are believed to be of roughly equal importance.[7] In the aqueous phase, numerous oxidants are known to participate in the S(IV)-to-S(VI) conversion. In the gas phase, the sole well-established SO_2 oxidant is the OH radical, which initiates a four-step reaction chain:[7]

$$SO_2 + OH \rightleftharpoons HSO_3 \quad (1)$$

$$HSO_3 + O_2 \rightleftharpoons HSO_5 \quad (2)$$

$$HSO_5 \rightleftharpoons SO_3 + HO_2 \quad (3)$$

$$SO_3 + (H_2O)_2 \rightleftharpoons H_2SO_4 + H_2O \quad (4)$$

As the HSO_5 intermediate is short-lived, reactions 2 and 3 can also be written as a single step. Because of the difference in ambient concentrations of OH, O_2, and H_2O, the rate-limiting step of the oxidation mechanism in the atmosphere is reaction 1, which has a rate constant of 1.3×10^{-12} cm^3 molecule^{-1} s^{-1} at 298 K and 1 atm.[8] The two other common atmospheric oxidants, O_3 and the NO_3 radical, react only very slowly with SO_2, and, therefore, do not contribute significantly to gas-phase H_2SO_4 production.[9] In a recent study,[10] we have shown mechanistically why this is the case for the NO_3 + SO_2 reaction. Sorokin[11] has proposed that excited-state oxygen molecules (singlet b state, formed by visible absorption) could play a role in SO_2 oxidation. However, as the exothermic reaction yielding O (^{3}P) is spin-forbidden, it is likely to be slow.

Nevertheless, field experiments[12] indicate the possible presence of a non-OH gas-phase sink of SO_2 and source of H_2SO_4. As this possible source seems to be present also at night, it is not likely to be photochemically driven, like, for example, the speculative spin-forbidden excited-state oxygen mechanism. We have investigated the possibility that two classes of organic oxidants, peroxyradicals and carbonyl oxides (Criegee intermediates), could play a role in gas-phase SO_2 oxidation. Both have been proposed as possible SO_2 oxidants by Wayne,[7] but

Received: April 27, 2011
Revised: June 22, 2011
Published: June 24, 2011

very few detailed studies on these reaction types have been carried out.

Peroxyradicals and Criegee intermediates are both reactive intermediates formed in the atmospheric oxidation of organic compounds. Peroxyradicals are generally formed by the addition of molecular oxygen (O_2) to radicals formed in hydrogen abstraction reactions by other oxidants, such as OH or NO_3

$$RH + OH \Rightarrow R + H_2O \quad (5)$$

$$R + O_2 \Rightarrow ROO \quad (6)$$

where R is any organic functional group (or hydrogen). For example, the methyl peroxyradical CH_3OO is formed in the oxidation of methane. Peroxyradicals undergo a variety of different reactions, the most important being the reaction with NO to produce NO_2 and an oxyradical. In low-NO_x conditions, recombination reactions with other radicals are also significant sinks for peroxyradicals.[7]

The reaction of HO_2 with SO_2 has been studied both experimentally and theoretically. A theoretical study by Wang and Hou[13] using B3LYP/aug-cc-pV(T+d)Z geometries and CCSD(T)/aug-cc-pV(T+d)Z single-point energies found a high (around 10 kcal/mol) barrier for the $SO_2 + HO_2 \Rightarrow SO_3 + OH$ reaction and also found that the reaction is unable to compete with the endothermic, but barrierless, formation of $HSO_2 + O_2$. The high barrier is in agreement with experimental results by Graham et al.,[14] who reported an upper limit of 1×10^{-18} cm^3 $molecule^{-1}$ s^{-1} for the $SO_2 + HO_2$ reaction.

The reaction of methyl peroxyradicals with SO_2 has been studied experimentally in the late 1970s and early 1980s and was, for a period of time, the subject of some controversy. Kan et al.[15] and Sanheuza et al.[16] studied the $SO_2 + CH_3OO$ reaction and found it to be reasonably fast, with reported rate constants on the order of 10^{-14} cm^3 $molecule^{-1}$ s^{-1}. However, in 1981, Sander and Watson[17] reinvestigated the system and reported an upper limit of 5×10^{-17} cm^3 $molecule^{-1}$ s^{-1}. This latter rate constant indicates that the reaction is too slow compared to other SO_2 and CH_3OO sink reactions to play any role in the atmosphere. Similar results were also reported in later investigations by Kan et al.[18] and Cocks et al.[19] The main reason for the discrepancies between the studies has been assumed to be the reversible formation of a SO_2-CH_3OO adduct, and the effect of various aspects of the experimental setup on the fate of this adduct. The SO_2-CH_3OO adduct has also been speculated to react with O_2 and NO, either forming further adducts or promoting decomposition, and Cocks et al.[19] further report a "stabilizing influence by the presence of water".

Cocks et al.[19] directly monitored the loss of SO_2 rather than CH_3OO as in the previous studies and found that the formation of SO_3 only proceeds via another CH_3OO radical reacting with the adduct to yield $SO_3 + CH_3O + CH_3OO$. This pathway was only competitive with decomposition at artificially high radical concentrations. The central conclusion of all the latter studies, as well as more modern reaction rate compilations,[9] was that the net formation rate of SO_3 is very low at radical concentrations corresponding to those found in the troposphere.

Criegee intermediates (CIs), also called Criegee biradicals due to their partial biradical character, are formed in the reactions of ozone with unsaturated organic compounds:

$$R_1R_2C{=}CR_3R_4 + O_3 \Rightarrow R_1R_2C(O_3)CR_3R_4 \quad (7)$$

$$R_1R_2C(O_3)CR_3R_4 \Rightarrow R_1R_2COO + R_3R_4CO \quad (8)$$

Here, $R_1...R_4$ denote arbitrary functional groups, $R_1R_2C(O_3)CR_3R_4$ denotes a short-lived primary ozonide (with a five-membered C−O−O−O−C ring), R_1R_2COO is a Criegee intermediate, and R_3R_4CO an aldehyde or ketone. Because reaction 8 is extremely exothermic, the CIs are formed with a large amount of excess vibrational energy. They may undergo either unimolecular isomerization or decomposition reactions, or be collisionally stabilized, forming stabilized Criegee intermediates (SCIs). The fraction of CIs that are stabilized depends on the size and nature of the functional groups R_1 and R_2, with larger CIs tending to be more easily stabilized. SCIs are known to react with a large number of organic and inorganic species, and estimates of their ambient concentrations vary widely. Though the existence of CIs was postulated as early as 1944,[20] they have only very recently been observed experimentally.[21] An important feature of the chemistry of CIs is that some of their reactions form OH radicals. This is one of the major sources of OH at night, when the normal photochemical OH production mechanism is absent.[7]

In 1985, Calvert et al.[22] suggested that gas-phase oxidation of SO_2 by methyl carbonyl oxide (CH_2OO) may be significant in polluted conditions, though measurements by Hatakeyama et al.[23] yielded only a rather low rate coefficient of $(4.9 \pm 2.0) \times 10^{-15}$ cm^3 $molecule^{-1}$ s^{-1} for the $SO_2 + CH_2OO$ reaction. This rate coefficient is similar to more recent results by Johnson et al.,[24] who reported an upper limit for the rate constant of the bimolecular reaction of ethyl and propyl carbonyl oxides [*syn*-CH_3CHOO, *anti*-CH_3CHOO, and $(CH_3)_2COO$] with SO_2 of 4×10^{-15} cm^3 $molecule^{-1}$ s^{-1}. It should be noted that experimental determinations of bimolecular rate constants for CIs are, in general, strongly dependent on assumptions or measurements of the lifetime of the SCIs with respect to unimolecular decomposition. For example, the rate coefficients of Johnson et al. are based on SCI lifetimes reported by Kroll et al.[25]

The reaction of the one-carbon Criegee intermediate CH_2OO (methyl carbonyl oxide) with SO_2 has been theoretically studied by Aplincourt and Ruiz-Lopez[26] and by Jiang et al.[27] In the former work, only the SO_2-catalyzed isomerization of CH_2OO into formic acid (HCOOH) was considered. Jiang et al. investigated both the isomerization and the oxidation of SO_2 to SO_3, with a focus on the reactions of large (nine carbon atoms) biogenic Criegee intermediates. Because of the large size of the systems they studied, Jiang et al were forced to use small basis sets in their study. They predicted that the transition states of all the oxidation reactions lie below the energy of the free reactants, but 14−23 kcal/mol above a strongly bound cyclic adduct intermediate. They used the B3LYP/6-31G(d,p) method to optimize the relevant stationary points and calculated single-point energies with CCSD(T) theory using the small 6-31G(d,p) basis set, with a basis set correction from 6-31G(d,p) to 6-311G(d,p) obtained with MP2. However, MP2-level basis set effects for ozonolysis products, such as the Criegee intermediate, may not always be transferable to higher-order methods, such as CCSD(T).[28] Second, even the 6-311G(d,p) basis set contains only one set of *d*-functions and may be insufficient for describing the bonding patterns of the hypervalent (i.e., possessing more than four bonds in the Lewis structures) sulfur atoms in the reaction adducts, transition states, and the SO_3 molecule.

Our objective is to systematically characterize the oxidation of SO_2 to SO_3 by organic oxidants in the atmosphere. Our focus is two-fold. First, we investigate whether larger substituents or water catalysis could speed up the peroxyradical + SO_2 reaction enough to play a role in the atmosphere. Second, we investigate the reaction of two Criegee intermediates with SO_2 and compare results for the two classes of organic oxidants.

2. COMPUTATIONAL DETAILS

Geometries and vibrational frequencies for all species in this study were computed with the density functional B3LYP[29,30] and the aug-cc-pV(T+d)Z basis set,[31] which is identical to the standard aug-cc-pVTZ basis set for first-row atoms but contains an extra set of tight *d*-functions for the second-row atoms. These extra basis functions have been shown to significantly improve the description of bonding to sulfur atoms.[32] As shown by Wang and Hou,[13] the use of smaller basis sets for the SO_2 + HO_2 system may lead to qualitative errors. Presumably, this applies also to the reactions of SO_2 with larger peroxyradicals.

Single-point energies at the B3LYP geometries have been calculated using the explicitly correlated coupled cluster singles, doubles, and perturbative triples method CCSD(T)-F12a/VDZ-F12.[33,34] The default CCSD-F12 correlation factor $[(1/\beta)\exp(-\beta r_{12})$, where $\beta = 1]$ was used in all explicitly correlated calculations. The inclusion of explicit electron−electron correlation greatly increases the proportion of correlation energy recovered with a given basis set.[35] Recent benchmark studies have shown that reaction barriers obtained with the CCSD(T)-F12a method using a given basis set are comparable to results obtained with conventional CCSD(T) using a basis set two cardinal numbers higher;[36,37] for example, CCSD(T)-F12a/VDZ-F12 results are comparable to CCSD(T)/aug-cc-pVQZ results. The VDZ-F12 orbital basis set used in the CCSD(T)-F12 calculations has been specifically optimized for use with explicitly correlated F12 methods and is of a similar size to the equivalent aug-cc-pVDZ and aug-cc-pV(D+d)Z basis sets. Density fitting approximations[38,39] and the resolution of the indentity (RI) approximation were utilized in all explicitly correlated calculations with the default auxiliary basis sets.[40−42] Of the two different approximations available for solving the CCSD(T)-F12 energies, we have used the CCSD(T)-F12a variant. The CCSD(T)-F12a method is recommended for double-ζ orbital basis sets,[43] and test calculations during this and previous studies[44] indicate that relative energies calculated with the two different F12 methods vary by 1 kcal mol^{-1} or less.

All species with an unpaired number of electrons, as well as the Criegee intermediates, were treated using the spin-unrestricted methods UB3LYP and UCCSD(T)-F12. The UCCSD(T)-F12 calculations were based on a restricted open-shell Hartree−Fock (ROHF) reference. In a previous study[10] on the addition−elimination reaction of NO_3 with four sulfur-containing molecules, including SO_2, we have shown that the barrier heights predicted by the approach used here are in good agreement with multireference methods, such as CASSCF and MRCI. Also, Cremer et al. have shown that, despite the partial multireference character of Criegee intermediates, DFT and CCSD(T) yield reasonably accurate results on their reactions.[45] The T1 diagnostic values for the CCSD(T)-F12a/VDZ-F12 single-point energies cover the range of 0.0008−0.053 and are typically 0.02−0.03. This indicates that the multireference character of the stationary points is only modest, and hence, the CCSD(T)-F12a method should provide a reasonable description of the reaction energetics.

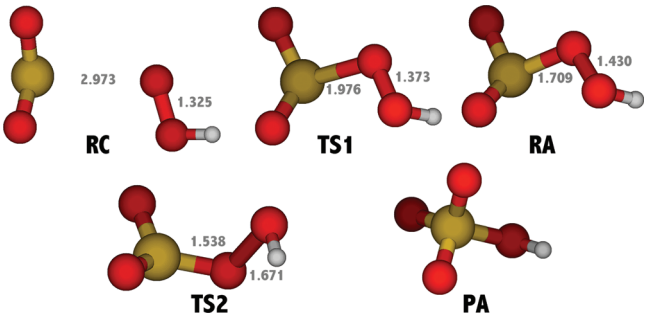

Figure 1. Stationary points of the SO_2 + HO_2 reaction, at the UB3LYP/aug-cc-pV(T+d)Z level. Color coding: yellow = sulfur, red = oxygen, white = hydrogen. Relevant interatomic distances are given in angstroms.

For the reaction of HO_2 with SO_2, and for the isomerization reaction of CH_2OO with SO_2, the stationary points found in previous studies[13,22] were used as trial geometries. For the other systems, S−O, O−O, and O−C distances and S−O−O and O−O−C angles from previously studied systems were used as trial geometries, and further configurational searching was carried out via potential energy scans, mainly with the S−O bond lengths as the variable parameters. For all transition states (species with one imaginary vibrational frequency), IRC calculations were performed at the B3LYP/aug-cc-pV(T+d)Z level to confirm that the presented reaction and product complexes were indeed connected to the transition state.

The Cartesian coordinates of all studied structures, optimized at the B3LYP/aug-cc-pV(T+d)Z level, as well as computed absolute energies, enthalpies, and free energies are given in the Supporting Information. Visualizations of molecular structures and orbitals were carried out using the MOLDEN program.[46] The aug-cc-pV(X+d)Z basis sets used in this study were obtained from the EMSL basis set exchange.[47] B3LYP calculations were carried using the Gaussian 09 program suite,[48] whereas CCSD(T)-F12 calculations were carried out using Molpro 2010.1.[49] Default energy and geometry convergence criteria were used. Thermal contributions to enthalpies and free energies were computed using the standard rigid rotor and harmonic oscillator approximations.

3. RESULTS AND DISCUSSION

3.1. RO_2 + SO_2 Reaction. The stationary points identified for the reaction of SO_2 with HO_2 are shown in Figure 1. The corresponding reaction energies, enthalpies, and free energies are given in Table 1. The energy profile of the reaction path of this and subsequent SO_2 + RO_2 reaction paths are shown in Figure 2. Unless otherwise specified, relative energies referred to in the discussion correspond to CCSD(T)-F12a/VDZ-F12 single-point energies of the corresponding B3LYP/aug-cc-pV(T+d)Z optimized stationary points. The reaction proceeds similarly to the SO_2 + NO_3 oxygen-transfer reaction studied previously.[10] First, a weakly bound reactant complex (RC) is formed. This complex is connected by an IRC path to the first transition state (TS1). The imaginary vibrational mode of TS1 corresponds to the formation of a S−O single bond and a simultaneous elongation of the O−O bond. TS1 is connected on the product

dx.doi.org/10.1021/jp203907d |J. Phys. Chem. A 2011, 115, 8669–8681

Table 1. Energetics of the SO_2 + HO_2 Reaction, in kcal/mol, with Respect to Free Reactants[a]

	ΔE_{elec}, B3LYP	ΔE_{elec}, CCSD(T)	ΔH, B3LYP	ΔG, B3LYP	ΔG^*, CCSD(T)
RC	−2.0	−2.7	−0.7	+5.4	+4.6
TS1	+6.3	+9.1	+7.1	+18.1	+20.9
RA	+4.3	+2.4	+6.0	+17.1	+15.2
TS2	+13.2	+11.3	+13.6	+24.5	+22.6
PA	−43.3	−50.3	−41.6	−29.5	−36.6
SO_3 + OH	−11.5	−18.4	−11.8	−8.8	−15.7

[a] B3LYP corresponds to UB3LYP/aug-cc-pV(T+d)Z, whereas CCSD(T) corresponds to UCCSD(T)-F12a/VDZ-F12 energies at the UB3LYP/aug-cc-pV(T+d)Z geometries. The "ΔG^*, CCSD(T)" column refers to free energies computed by combining the UCCSD(T)-F12a/VDZ-F12 electronic energies with the B3LYP zero-point energies and thermal free energy contributions. All enthalpy and free energy values are computed at 298.15 K and 1 atm reference pressure.

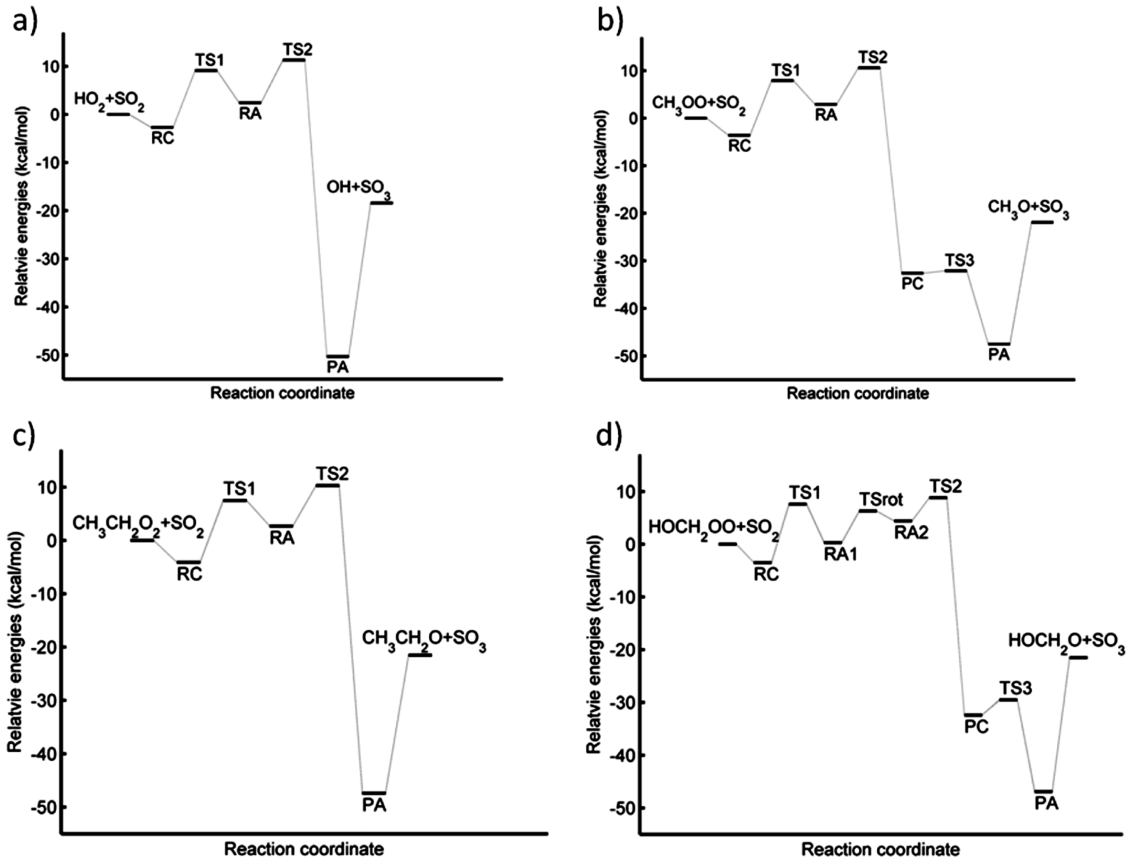

Figure 2. CCSD(T)-F12a/VDZ-F12//B3LYP/aug-cc-pV(T+d)Z energy profile of the reactions of SO_2 with four different peroxyradicals: (a)SO_2 + HO_2, (b)SO_2 + CH_3OO, (c) SO_2 + CH_3CH_2OO, (d)SO_2 + $HOCH_2OO$.

side to an intermediate reaction adduct (RA), which is around 6.7 kcal/mol lower in energy. The adduct, in turn, reacts further via a second transition state (TS2). The imaginary vibrational mode of TS2 corresponds to the breaking of the O−O bond and the simultaneous contraction of the S−O bond. The IRC path from TS2 forward is rather complicated. Immediately after the O−O bond breaks, a SO_3 + OH complex is formed. However, this complex does not correspond to a minimum on the B3LYP/aug-cc-pV(T+d)Z potential energy surface but reacts directly (no barrier) to give the HSO_4 radical product adduct (denoted "PA"). Our structural and thermodynamic results are essentially identical to those given by Wang and Hou,[13] except that we additionally find the TS1 and RA stationary points. In terms of the final kinetics of the reaction, this is of lesser importance as TS2 represents the rate-limiting step, lying about 11 kcal/mol above the free reactants in energy.

The first steps of the SO_2 + CH_3OO reaction are both structurally and energetically similar to those of the SO_2 + HO_2 reaction, as shown in Figure 3 and Table 2. However, the second transition state leads to a SO_3 + CH_3O product complex (PC), which must cross a further small energy barrier corresponding to the transition state TS3 to form a CH_3OSO_3 product adduct (PA). The PC to TS3 barrier is much lower than the energy required to dissociate the PC into SO_3 + CH_3O, which is more than 10 kcal/mol. Given this, as well as the strong exothermicity of the conversion of RA to PC through TS2, the

TS3 transition state will likely not play any role for the real reaction dynamics, as the formed complex has more than enough excess energy to cross the 0.5 kcal/mol barrier. As with the SO_2 + HO_2 (and SO_2 + NO_3)[10] reaction, the rate-limiting step corresponds to TS2, which lies 10.6 kcal/mol above the free reactants.

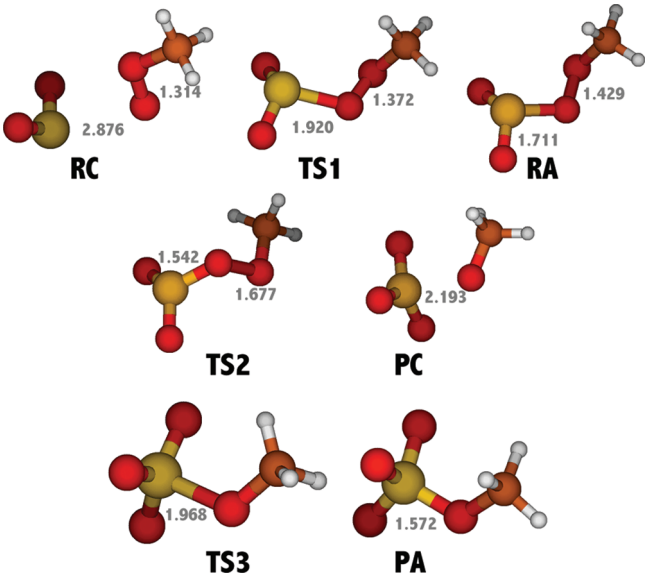

Figure 3. Stationary points of the SO_2 + CH_3OO reaction, at the UB3LYP/aug-cc-pV(T+d)Z level. Color coding: yellow = sulfur, red = oxygen, brown = carbon, white = hydrogen. Relevant interatomic distances are given in angstroms.

The computed results are in qualitative agreement with experimental results,[19] both concerning the existence of intermediate complexes and adducts and in the conclusion that the reaction is too slow to play a role in the atmosphere.

Next, we investigated how the replacement of a hydrogen atom in CH_3OO by a methyl group or a hydroxyl group affects the ability of the peroxyradical to oxidize SO_2. The energetics and structural characteristics of the SO_2 + CH_3CH_2OO reaction (see Table 3 and Figure 2) are very similar to those of the SO_2 + HO_2 reaction, and the corresponding stationary points are, therefore, not displayed (see the Supporting Information for Cartesian coordinates). Similar to the SO_2 + HO_2 reaction, TS2 of the SO_2 + CH_3CH_2OO reaction leads directly to a $CH_3CH_2OSO_3$ radical product adduct, rather than to a SO_3 + CH_3CH_2O complex. Thus, it seems that extending the carbon chain has little effect on the reaction with SO_2.

The stationary points of the SO_2 + $HOCH_2OO$ reaction (see Figure 4 and Table 4) are somewhat different from the previous reactions. First, the reactant complex (RC) contains a weak COH···O═S hydrogen bond rather than a COO···S interaction. This hydrogen bond is broken in the formation of the TS1 transition state. Instead of one intermediate reaction adduct, the SO_2 + $HOCH_2OO$ reaction path contains two (RA1 and RA2). These are connected by a transition state (TSrot) corresponding to the rotation of the OH group to reform the COH···O═S hydrogen bond. Hindered rotor calculations on RA1 and RA2 indicate that the OH group rotation is best described as a hindered internal rotation. Thus, TSrot may not be a true stationary state but an artifact of the harmonic oscillator model. On the other hand, even after hindered rotor corrections, the free

Table 2. Energetics of the SO_2 + CH_3OO Reaction, in kcal/mol, with Respect to Free Reactants[a]

	ΔE_{elec}, B3LYP	ΔE_{elec}, CCSD(T)	ΔH, B3LYP	ΔG, B3LYP	ΔG^*, CCSD(T)
RC	−2.8	−3.6	−1.5	+4.6	+3.8
TS1	+6.4	+7.9	+6.9	+18.4	+20.0
RA	+5.3	+2.9	+6.7	+18.2	+15.7
TS2	+12.5	+10.6	+12.6	+24.0	+22.1
PC	−26.8	−32.6	−26.0	−15.9	−21.7
TS3	−26.5	−32.1	−26.1	−14.1	−19.7
PA	−38.9	−47.5	−37.0	−24.4	−33.0
SO_3 + CH_3O	−17.7	−21.9	−18.8	−17.2	−21.3

[a] B3LYP corresponds to UB3LYP/aug-cc-pV(T+d)Z, whereas CCSD(T) corresponds to UCCSD(T)-F12a/VDZ-F12 energies at the UB3LYP/aug-cc-pV(T+d)Z geometries. The "ΔG^*, CCSD(T)" column refers to free energies computed by combining the UCCSD(T)-F12a/VDZ-F12 electronic energies with the B3LYP zero-point energies and thermal free energy contributions. All enthalpy and free energy values are computed at 298.15 K and 1 atm reference pressure.

Table 3. Energetics of the SO_2 + CH_3CH_2OO Reaction, in kcal/mol, with Respect to Free Reactants[a]

	ΔE_{elec}, B3LYP	ΔE_{elec}, CCSD(T)	ΔH, B3LYP	ΔG, B3LYP	ΔG^*, CCSD(T)
RC	−3.0	−4.1	−1.7	+5.5	+4.4
TS1	+6.6	+7.5	+7.2	+18.8	+19.8
RA	+5.7	+2.7	+7.0	+18.6	+15.7
TS2	+12.6	+10.3	+12.6	+24.2	+21.8
PA	−38.2	−47.4	−36.3	−24.0	−33.1
SO_3 + CH_3CH_2O	−17.6	−21.5	−18.9	−18.0	−21.9

[a] B3LYP corresponds to UB3LYP/aug-cc-pV(T+d)Z, whereas CCSD(T) corresponds to UCCSD(T)-F12a/VDZ-F12 energies at the UB3LYP/aug-cc-pV(T+d)Z geometries. The "ΔG^*, CCSD(T)" column refers to free energies computed by combining the UCCSD(T)-F12a/VDZ-F12 electronic energies with the B3LYP zero-point energies and thermal free energy contributions. All enthalpy and free energy values are computed at 298.15 K and 1 atm reference pressure.

energies of RA1 and RA2 are different by a few kcal/mol (see the Supporting Information), indicating that they may be distinct minima despite being connected by a hindered rotation. As none of these stationary points correspond to the rate-limiting step of the overall reaction, these details do not affect the overall assessment of the reaction rate. RA2 is connected on the product side to TS2, which lies about 8.8 kcal/mol above the reactants in energy. From TS2 onward, the reaction proceeds analogously to the SO_2 + CH_3OO reaction, with a low barrier connecting the product complex to a product adduct.

The rate-limiting barrier for the reaction of SO_2 with all four studied peroxyradicals is around 9−11 kcal/mol with respect to the CCSD(T)-F12 energies, or around 20−23 kcal/mol with respect to the free energies computed using CCSD(T)-F12 electronic energies and B3LYP zero-point energy and thermal contributions. Within the framework of elementary transition-state theory, this implies reaction rate constants of well below 5×10^{-21} cm^3 $molecule^{-1}$ s^{-1}. Thus, the reactions of any peroxyradicals with SO_2 are unlikely to contribute significantly to SO_2 oxidation anywhere in the atmosphere. However, our result that the reactions of peroxyradicals with SO_2 proceed directly to an organosulfate radical adduct may possibly help explain the field observation[50] of small amounts of organosulfate anions (with the empirical formula $C_2H_3SO_6^-$) in the gas phase. As organosulfates have extremely low vapor pressures, the observed $C_2H_3SO_6^-$ anions likely have a gas-phase source. Despite its low yield, the SO_2 + peroxyradical reaction might be one such source, though the mechanism by which the formed radical evolves into a stable closed-shell organosulfate (a strong acid, which then easily deprotonates to form the anion) remains speculative.

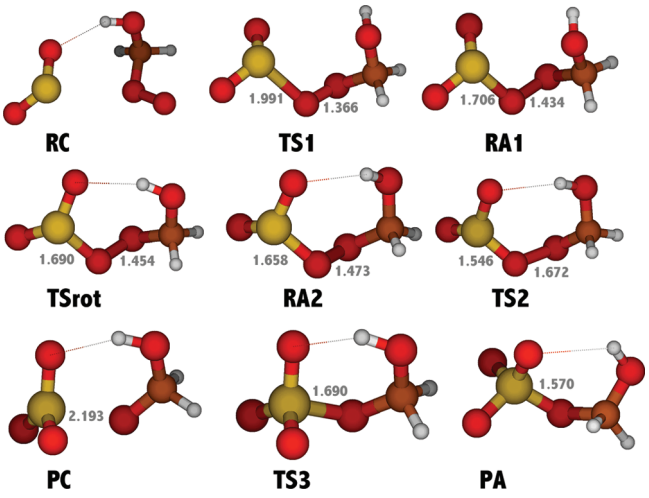

Figure 4. Stationary points of the SO_2 + $HOCH_2OO$ reaction, at the UB3LYP/aug-cc-pV(T+d)Z level. Color coding: yellow = sulfur, red = oxygen, brown = carbon, white = hydrogen. Relevant interatomic distances are given in angstroms.

3.2. Effect of Water Catalysis: SO_2 + $HO_2 \cdot H_2O$ and $HOCH_2OO \cdot H_2O$. Water catalysis is known to significantly speed up many atmospheric oxidation reactions, such as DMS + OH,[51] HCOOH + OH,[52] and CH_3CHO + OH.[53] For water catalysis to play a role in the atmosphere, two criteria must be met. First, at least one of the reactants must bind to water strongly enough for the hydrated complex to have a reasonable atmospheric abundance. For typical trace gases with concentrations in the high parts per billion range, this usually corresponds to Gibbs free energies of hydration of −1 kcal/mol or lower. For example, at a temperature of 298 K and a relative humidity of 100%, a Gibbs free energy of hydration of −1 kcal/mol implies that about 14% of the molecules in question are hydrated. Second, the presence of a water molecule must allow for a different (lower-energy) reaction path or hydration must lower the energy of the transition state more than that of the reactants. The Gibbs free energy of the hydration of SO_2 is around +3 kcal/mol,[54] and $SO_2 \cdot H_2O$ can, therefore, be ruled out as a reactant. Thus, results for $SO_2 \cdot H_2O$ + RO_2 reactions are not shown. Of the four peroxyradicals studied here, only HO_2 and $HOCH_2OO$ form even moderately strongly bound hydrates, with zero-point-corrected binding energies of around 7 and 5 kcal/mol, respectively.[55] Both CH_3OO and CH_3CH_2OO bind too weakly to water for their hydrates to be found in appreciable amounts in the atmosphere. The binding energies of the CH_3OO and CH_3CH_2OO hydrates are around 2.5 kcal/mol, implying Gibbs free energies of hydration well above zero.[57]

The stationary points for the SO_2 + $HO_2 \cdot H_2O$ and SO_2 + $HOCH_2OO \cdot H_2O$ reactions are shown in Figures 5 and 6, respectively, with the corresponding energetic data given in Tables 5 and 6, respectively. The mechanism of the SO_2 + $HO_2 \cdot H_2O$ reaction is identical to its unhydrated counterpart. The presence of water lowers the energy of TS2 insignificantly.

Table 4. Energetics of the SO_2 + $HOCH_2OO$ Reaction, in kcal/mol, with Respect to Free Reactants[a]

	ΔE_{elec}, B3LYP	ΔE_{elec}, CCSD(T)	ΔH, B3LYP	ΔG, B3LYP	ΔG^*, CCSD(T)
RC	−2.1	−3.5	−0.8	+5.6	+4.2
TS1	+6.0	+7.6	+6.5	+18.0	+19.6
RA1	+3.4	+0.3	+4.8	+16.7	+13.6
TSrot	+9.1	+6.3	+9.3	+21.4	+18.6
RA2	+7.7	+4.4	+8.8	+20.4	+17.0
TS2	+10.8	+8.8	+10.6	+22.6	+20.6
PC	−29.3	−32.4	−29.4	−18.6	−21.7
TS3	−27.2	−29.5	−28.0	−14.8	−17.1
PA	−38.3	−46.9	−36.5	−24.0	−32.5
SO_3 + $HOCH_2O$	−21.5	−23.8	−22.9	−21.9	−24.2

[a] B3LYP corresponds to UB3LYP/aug-cc-pV(T+d)Z, whereas CCSD(T) corresponds to UCCSD(T)-F12a/VDZ-F12 energies at the UB3LYP/aug-cc-pV(T+d)Z geometries. The "ΔG^*, CCSD(T)" column refers to free energies computed by combining the UCCSD(T)-F12a/VDZ-F12 electronic energies with the B3LYP zero-point energies and thermal free energy contributions. All enthalpy and free energy values are computed at 298.15 K and 1 atm reference pressure.

The presence of water makes the mechanism of the SO_2 + $HOCH_2OO\cdot H_2O$ somewhat simpler. Because the COH group is constantly hydrogen bonded to water rather than to the S═O oxygen, the intermediate transition state TSrot is absent. Otherwise, the reactions with and without water are qualitatively similar. The energy of the rate-limiting TS2 transition state is actually somewhat higher for the reaction involving the hydrate; +9.7 kcal/mol compared to +8.8 kcal/mol for the unhydrated reaction. The effect of water on the SO_2 + RO_2 reaction rate is thus likely to be negligible.

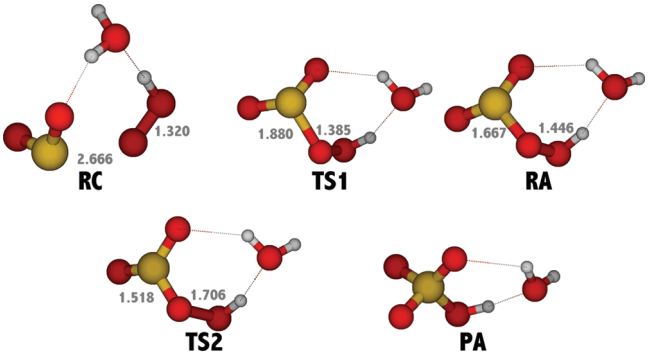

Figure 5. Stationary points of the SO_2 + $HO_2\cdot H_2O$ reaction, at the UB3LYP/aug-cc-pV(T+d)Z level. Color coding: yellow = sulfur, red = oxygen, brown = carbon, white = hydrogen. Relevant interatomic distances are given in angstroms.

In structural terms, the lack of significant water catalysis on the studied reactions is fairly easy to understand. Strongly water-catalyzed reactions are often hydrogen or proton transfers, where the presence of water may allow for a qualitatively different reaction path, such as that observed in a recent study on water- and acid-catalyzed methoxyradical isomerization.[56] For example, the catalyzing water molecule may simultaneously accept and donate a hydrogen atom, and the barrier for this process may be much lower than for the original direct hydrogen transfer. Alternatively, the structure of the transition state may be such that it is able to form much stronger H-bonds with water than either of the reactants. The SO_2 oxidation reactions studied here are essentially oxygen transfers, where the second oxygen on a C−O−O group is donated to a sulfur atom. Unlike hydrogen or proton transfers, the presence of water does not open up alternative reaction pathways for oxygen transfers. Furthermore, since neither the peroxide group oxygen atoms, the S═O oxygen atoms, nor the sulfur atom form particularly strong hydrogen bonds to water, the water molecule is unable to significantly stabilize the transition state with respect to free SO_2 and the hydrated peroxides. These two characteristics lead to little or no water catalysis for the studied reaction types.

3.3. Potential Contribution of Electronically Excited Peroxyradicals. Peroxyradicals are known to have electronic transitions corresponding to both ultraviolet and near-infrared radiation. Even if the thermal reactions of peroxyradicals with SO_2 are slow, as shown above, electronically excited peroxyradicals could still conceivably contribute to SO_2 oxidation. This

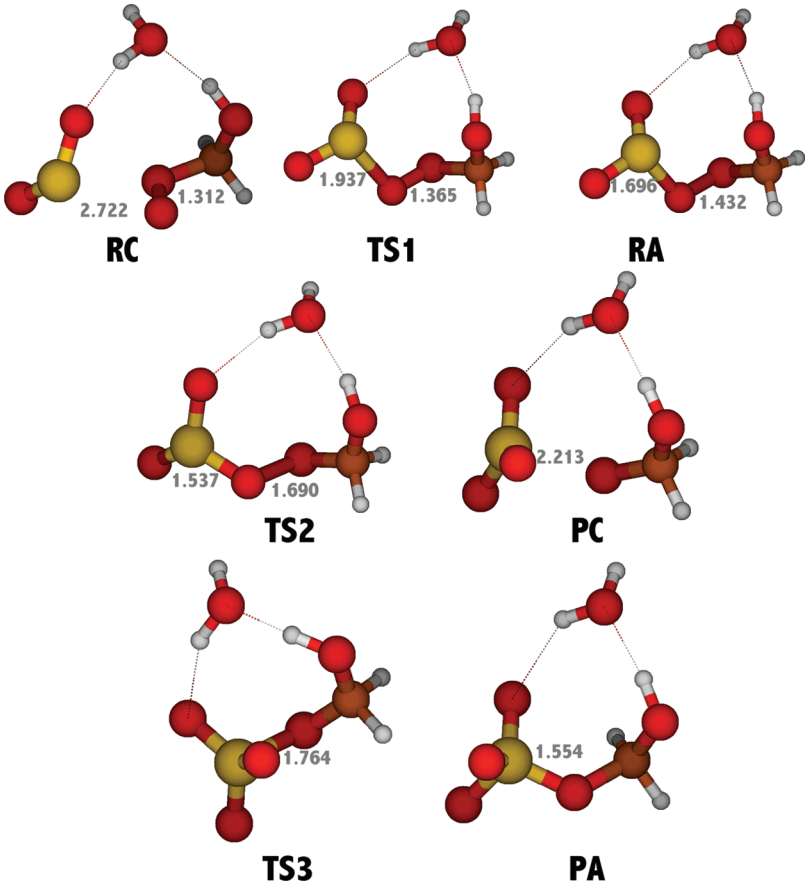

Figure 6. Stationary points of the SO_2 + $HOCH_2OO\cdot H_2O$ reaction, at the UB3LYP/aug-cc-pV(T+d)Z level. Color coding: yellow = sulfur, red = oxygen, brown = carbon, white = hydrogen. Relevant interatomic distances are given in angstroms.

dx.doi.org/10.1021/jp203907d |J. Phys. Chem. A 2011, 115, 8669–8681

Table 5. Energetics of the SO_2 + $HO_2 \cdot H_2O$ Reaction, in kcal/mol, with Respect to Free Reactants (SO_2 and the $HO_2 \cdot H_2O$ Complex)[a]

	ΔE_{elec}, B3LYP	ΔE_{elec}, CCSD(T)	ΔH, B3LYP	ΔG, B3LYP	ΔG^*, CCSD(T)
RC	−7.0	−6.8	−5.7	+4.1	+4.3
TS1	+7.4	+8.0	+8.1	+19.8	+20.4
RA	+6.1	+3.2	+7.5	+19.2	+16.2
TS2	+13.6	+10.7	+13.8	+25.7	+22.8
PA	−46.3	−53.9	−44.8	−31.9	−39.5

[a] B3LYP corresponds to UB3LYP/aug-cc-pV(T+d)Z, whereas CCSD(T) corresponds to UCCSD(T)-F12a/VDZ-F12 energies at the UB3LYP/aug-cc-pV(T+d)Z geometries. The "ΔG^*, CCSD(T)" column refers to free energies computed by combining the UCCSD(T)-F12a/VDZ-F12 electronic energies with the B3LYP zero-point energies and thermal free energy contributions. All enthalpy and free energy values are computed at 298.15 K and 1 atm reference pressure.

Table 6. Energetics of the SO_2 + $HOCH_2OO \cdot H_2O$ Reaction, in kcal/mol, with Respect to Free Reactants (SO_2 and the $HOCH_2OO \cdot H_2O$ Complex)[a]

	ΔE_{elec}, B3LYP	ΔE_{elec}, CCSD(T)	ΔH, B3LYP	ΔG, B3LYP	ΔG^*, CCSD(T)
RC	−3.4	−4.4	−2.3	+6.0	+5.0
TS1	+4.2	+4.9	+4.7	+16.8	+17.4
RA	+2.3	−1.6	+3.6	+15.8	+11.9
TS2	+10.8	+9.7	+10.4	+22.0	+20.9
PC	−28.0	−31.8	−28.2	−17.3	−21.1
TS3	−26.7	−28.5	−28.3	−14.2	−16.0
PA	−38.4	−47.0	−36.7	−24.9	−33.5

[a] B3LYP corresponds to UB3LYP/aug-cc-pV(T+d)Z, whereas CCSD(T) corresponds to UCCSD(T)-F12a/VDZ-F12 energies at the UB3LYP/aug-cc-pV(T+d)Z geometries. The "ΔG^*, CCSD(T)" column refers to free energies computed by combining the UCCSD(T)-F12a/VDZ-F12 electronic energies with the B3LYP zero-point energies and thermal free energy contributions. All enthalpy and free energy values are computed at 298.15 K and 1 atm reference pressure.

mechanism would be analogous to the excited-oxygen mechanism proposed by Sorokin,[51] with the added benefit that the reaction of doublet excited-state peroxyradicals with singlet SO_2 to give singlet SO_3 and doublet oxyradicals is spin-allowed.

For small peroxyradicals,[57] the B ($^2A''$) ⟸ X ($^2A'$) electronic transition is unfortunately too high in energy (around 240 nm) to be of major importance in the troposphere, where the solar actinic flux below 290 nm is very small. Also, these transitions lead to almost immediate photolysis of the parent peroxyradical,[58] implying that the steady-state concentration of B state peroxyradicals available for bimolecular reactions is very low.

The A ($^2A'$) ⟸ X ($^2A'$) electronic transitions[59] in the near-infrared (NIR) region around 1300−1400 nm are more likely to enhance peroxyradical reactivity in the troposphere, as the solar actinic flux in the NIR region is high, though partially screened by water vapor absorption. Also, the A state is bound, indicating that the excited peroxyradicals might live long enough to participate in reactions. Conversely, the NIR transitions are quite weak, with cross sections around 10^{-20}−10^{-21} cm^{-2} $molecule^{-1}$, around 4−5 orders of magnitude lower than the (B ⟸ X) transition.[60] The participation of A state excited peroxyradicals in tropospheric chemistry has been proposed previously by Frost et al.,[61] though they focused on the enhancement by electronic excitation of unimolecular reaction, such as cyclization, followed by OH elimination. Frost et al. found that cross sections of around 10^{-18} cm^{-2} or higher are needed for the corresponding transitions to play a role in tropospheric chemistry. Recent measurements indicate that the real cross sections are around 2 orders of magnitude lower, for example, 2.7×10^{-20} cm^{-2} $molecule^{-1}$ for the methyl peroxyradical[57] and 5.3×10^{-21} cm^{-2} $molecule^{-1}$ for the ethyl peroxyradical.[62] This indicates that only a very small fraction of peroxyradicals in ambient conditions will live long enough to undergo photoexcitation to the A state. Furthermore, a large part of the few peroxyradicals that are excited will probably tend to react via unimolecular elimination channels before they collide with SO_2 molecules.[58] We can thus conclude that A state excited peroxyradicals are unlikely to play any major role in SO_2 oxidation.

If any of the reactant complexes or intermediate adducts described in the previous sections were strongly bound with respect to both directions on the reaction path, then electronic excitations of the complexes or adducts might influence the reactions. Some indications of this have been given by Cocks et al.[19] However, the complexes and intermediate adducts are generally bound by less than 5 kcal/mol with respect to the free reactants or the TS1 transition state, respectively. This indicates that their lifetimes with respect to evaporation or reverse reaction, respectively, are fairly short, and they will probably not have time to undergo electronic transitions in atmospheric conditions. Therefore, excitation of complexes or adducts is not investigated further here.

3.4. Reaction of SO_2 with Criegee Intermediates. The reaction of methyl carbonyl oxide (CH_2OO) with SO_2 can proceed via (at least) two different routes, as shown in Figure 7. The energy profile of both reactions is shown in Figure 8, with the energies given in Table 7. First, SO_2 can catalyze the strongly exothermic isomerization of CH_2OO to HCOOH, as shown by Aplincourt and Ruiz-Lopez.[22] Second, one of the CH_2OO oxygens can transfer to SO_2, forming SO_3 and CH_2O

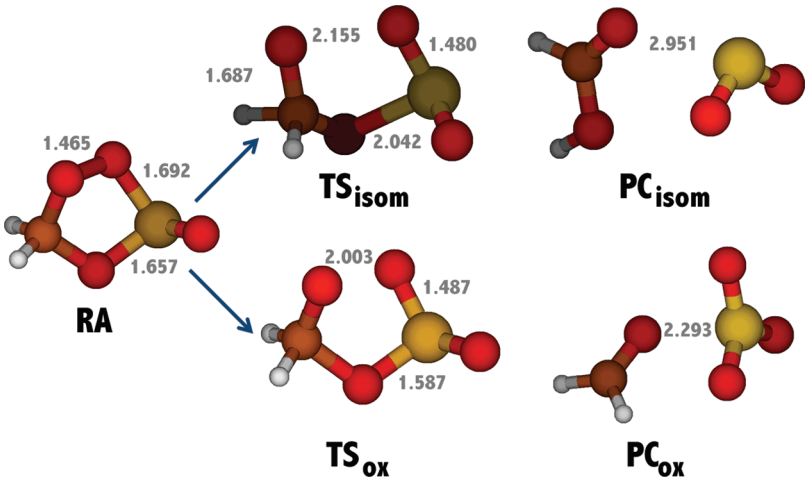

Figure 7. Stationary points of the SO_2 + CH_2OO reaction, at the UB3LYP/aug-cc-pV(T+d)Z level. Color coding: yellow = sulfur, red = oxygen, brown = carbon, white = hydrogen. Relevant interatomic distances are given in angstroms.

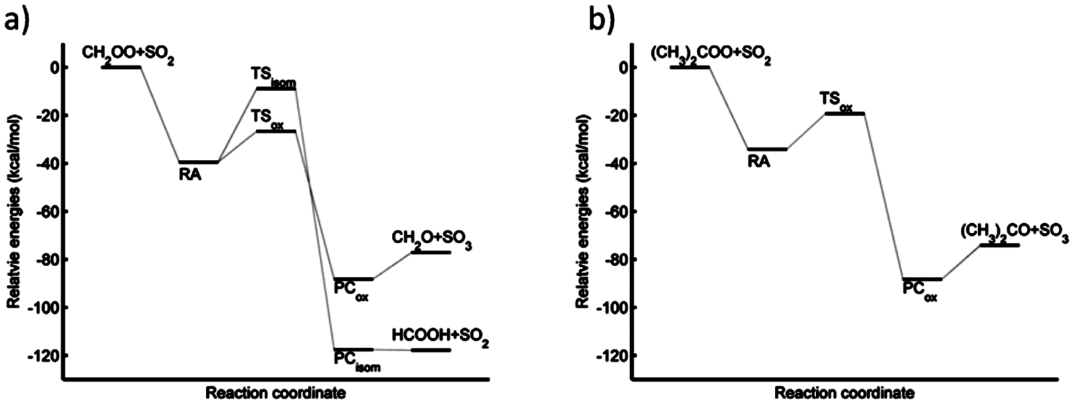

Figure 8. CCSD(T)- F12a/VDZ-F12//B3LYP/aug-cc-pV(T+d)Z energy profile of the reactions of SO_2 with two different Criegee intermediates: (a) SO_2 + CH_2OO and (b) SO_2 + $(CH_3)_2COO$.

Table 7. Energetics of the SO_2 + CH_2OO Reaction, in kcal/mol, with Respect to Free Reactants[a]

	ΔE_{elec}, B3LYP	ΔE_{elec}, CCSD(T)	ΔH, B3LYP	ΔG, B3LYP	ΔG^*, CCSD(T)
RA	−33.8	−39.5	−31.3	−18.1	−23.8
TS_{isom}	−4.2	−8.9	−5.4	+6.3	+1.6
PC_{isom}	−113.5	−117.6	−110.8	−104.9	−109.1
SO_2 + HCOOH	−114.5	−117.8	−113.0	−112.9	−116.2
TS_{ox}	−19.2	−26.6	−18.4	−5.4	−12.7
PC_{ox}	−79.5	−88.2	−77.3	−66.6	−75.2
SO_3 + CH_2O	−70.7	−77.1	−70.2	−69.1	−75.4

[a] B3LYP corresponds to UB3LYP/aug-cc-pV(T+d)Z, whereas CCSD(T) corresponds to UCCSD(T)-F12a/VDZ-F12 energies at the UB3LYP/aug-cc-pV(T+d)Z geometries. The "ΔG^*, CCSD(T)" column refers to free energies computed by combining the UCCSD(T)-F12a/VDZ-F12 electronic energies with the B3LYP zero-point energies and thermal free energy contributions. All enthalpy and free energy values are computed at 298.15 K and 1 atm reference pressure.

(formaldehyde), as shown by Jiang et al.[23] Both reactions proceed through the initial formation of a cyclic adduct (RA in Figure 7) that lies about 40 kcal/mol below the reactants. Both transition states are connected by IRC paths to the same cyclic adduct on the reactant side, and to (different) product complexes on the product side. The isomerization transition state TS_{isom} lies about 9 kcal/mol below the reactants in energy, and 1 kcal/mol above the reactants in free energy (ΔG^*). The imaginary vibrational mode of the isomerization transition state corresponds to the transfer of a hydrogen atom from the carbon atom to an oxygen atom, and the simultaneous breaking of the S−O bond. The oxidation transition state TS_{ox} is about 18 kcal/mol lower in energy, and its imaginary vibrational mode corresponds to the breaking of the C−O

dx.doi.org/10.1021/jp203907d |J. Phys. Chem. A 2011, 115, 8669–8681

and O−O bonds. The energy difference between the transition states, combined with the fact that the isomerization TS lies slightly above the reactants in free energy, indicates that the oxidation reaction should proceed significantly faster than the isomerization.

We find somewhat larger differences between the energies of the two transition states than in the study by Jiang et al.,[23] which mainly results from differences in the size of the basis set used for the geometry optimization and frequency calculations, as well as in the CCSD(T) energy calculations. For example, we find the reaction adduct and oxidation transition state to be 18.4 kcal/mol below the reactants in enthalpy at the B3LYP/aug-cc-pV(T+d)Z level, whereas Jiang et al. find it to be 11.1 kcal/mol below the reactants at the B3LYP/6-31G(d,p) level. Most of these differences may be caused by the inability of the 6-31G(d,p) or even the 6-311++G(d,p) basis sets to properly describe the binding of the sulfur atom, which becomes hypervalent in the reaction adducts and transition states and would thus presumably require multiple d orbitals to be modeled accurately. However, we emphasize that the qualitative description of the reaction pathways in our two studies are similar. This also serves to validate the qualitative results of Jiang et al. concerning the larger, nine-carbon SCIs, which would be unfeasible to calculate with our approach.

We have also studied the reaction of SO_2 with 2-propyl carbonyl oxide $(CH_3)_2OO$, which can be taken to be a representative example of larger (e.g., biogenic) Criegee intermediates. Because there is no hydrogen atom bound to the COO carbon atom, the SO_2-catalyzed isomerization pathway is not possible for this species. The oxidation reaction is qualitatively similar to that of the smaller SCI, as shown by Figure 9 and Table 8. Because of a greater degree of stabilization of the carbonyl oxide group by the adjacent carbon atoms, both the reactant adduct and the transition state are about 6−7 kcal/mol higher in relative energy than for the $CH_2OO + SO_2$ reaction. Despite this stabilization, the transition state is still 19.3 kcal/mol below the reactants in energy.

The overall oxidation reaction rates of SO_2 by the two Criegee intermediates can be estimated by assuming a pseudo steady state

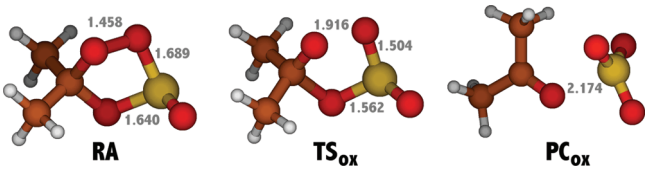

Figure 9. Stationary points of the $SO_2 + (CH_3)_2COO$ reaction, at the UB3LYP/aug-cc-pV(T+d)Z level. Color coding: yellow = sulfur, red = oxygen, brown = carbon, white = hydrogen. Relevant interatomic distances are given in angstroms.

for the CH_2OOSO_2 and $(CH_3)_2COOSO_2$ cyclic adducts

$$d[CH_2OOSO_2]/dt = k_{coll,1}[CH_2OO][SO_2] - k_{diss,1}[CH_2OOSO_2] - k_{ox,1}[CH_2OOSO_2] - k_{isom,1}[CH_2OOSO_2] \approx 0$$

$$[CH_2OOSO_2] = k_{coll,1}[CH_2OO][SO_2]/(k_{diss,1} + k_{ox,1} + k_{isom,1})$$

$$d[(CH_3)_2COOSO_2]/dt = k_{coll,3}[(CH_3)_2COO][SO_2] - k_{diss,3}[(CH_3)_2COOSO_2] - k_{ox,3}[(CH_3)_2COOSO_2] \approx 0$$

$$[(CH_3)_2COOSO_2] = k_{coll,3}[(CH_3)_2COO][SO_2]/(k_{diss,3} + k_{ox,3})$$

where k_{coll} refers to the collision rate of SO_2 and the Criegee intermediate that form the adduct, k_{diss} is the rate by which the adduct dissociates back to the reactants, and k_{ox} and k_{isom} are the rates by which the adducts cross the respective transition state. The subscripts 1 and 3 refer to the number of carbon atoms in the Criegee intermediate.

The overall oxidation reaction rate constant is then $(k_{ox,1} \times k_{coll,1})/(k_{diss,1} + k_{ox,1} + k_{isom,1})$ for the $CH_2OO + SO_2$ reaction and $(k_{ox,3} \times k_{coll,3})/(k_{diss,3} + k_{ox,3})$ for the $(CH_3)_2COO + SO_2$ reaction. The collision rates can be estimated from hard-sphere collision theory, yielding $k_{coll,1} \approx k_{coll,3} \approx 4 \times 10^{-10}$ cm^3 molecule^{-1} s^{-1} (with an uncertainty of some tens of percent depending on the assumed densities, and further uncertainties due to possible steric factors in the reaction mechanisms). From elementary transition-state theory (TST), and using CCSD(T)-F12 electronic energies together with B3LYP thermal contributions to estimate the activation free energies, we obtain the following: $k_{diss,1} \approx 2.1 \times 10^{-5}$ s^{-1}, $k_{ox,1} \approx 47\,000$ s^{-1}, $k_{isom,1} \approx 1.4 \times 10^{-6}$ s^{-1}, $k_{diss,3} \approx 0.28$ s^{-1}, and $k_{ox,3} \approx 1100$ s^{-1} at 298 K. This yields overall bimolecular reaction rate constants of very close to the assumed collision rate of 4×10^{-10} cm^3 molecule^{-1} s^{-1} for both the $CH_2OO + SO_2$ and the $(CH_3)_2COO + SO_2$ oxidation reactions. This approach assumes collisional stabilization of the adduct prior to crossing the transition state: if the adduct retains excess energy from the reactant collision, the rate of the $(CH_3)_2COO + SO_2$ reaction would likely be somewhat lower, as the dissociation of the adduct back to products would be faster.

Our TST estimated rate constant for the $(CH_3)_2COO + SO_2$ reaction is 5 orders of magnitude higher than the upper limit of 4×10^{-15} cm^3 molecule^{-1} s^{-1} predicted by Johnson et al.,[24] based on the very weak dependence of OH yields from ozonolysis on SO_2 concentrations. The difference may naturally be caused by computational errors. If the free energies and corresponding elementary rate constants were computed using

Table 8. Energetics of the $SO_2 + (CH_3)_2COO$ Reaction, in kcal/mol, with Respect to Free Reactants[a]

	ΔE_{elec}, B3LYP	ΔE_{elec}, CCSD(T)	ΔH, B3LYP	ΔG, B3LYP	ΔG^*, CCSD(T)
RA	−24.1	−34.1	−22.1	−8.2	−18.2
TS_{ox}	−8.8	−19.3	−8.1	+5.6	−4.9
PC_{ox}	−79.0	−88.3	−76.4	−65.8	−75.2
$SO_3 + (CH_3)_2O$	−67.8	−74.1	−66.9	−66.4	−72.7

[a] B3LYP corresponds to UB3LYP/aug-cc-pV(T+d)Z, whereas CCSD(T) corresponds to UCCSD(T)-F12a/VDZ-F12 energies at the UB3LYP/aug-cc-pV(T+d)Z geometries. The "ΔG^*, CCSD(T)" column refers to free energies computed by combining the UCCSD(T)-F12a/VDZ-F12 electronic energies with the B3LYP zero-point energies and thermal free energy contributions. All enthalpy and free energy values are computed at 298.15 K and 1 atm reference pressure.

dx.doi.org/10.1021/jp203907d |J. Phys. Chem. A 2011, 115, 8669–8681

B3LYP electronic energies instead of CCSD(T)-F12 electronic energies, the final reaction rate for the $(CH_3)_2COO + SO_2$ reaction would be about 4 orders of magnitude lower. While the CCSD(T)-F12 energies can definitely be assumed to be more reliable than the B3LYP energies, this huge difference nevertheless illustrates that the obtained rate constants are quite sensitive to the employed computational method. To check whether the CCSD(T)-F12a/VDZ-F12 energies are significantly contaminated by basis-set incompleteness error, we recomputed the $(CH_3)_2COO + SO_2$ reaction adduct and transition-state energies using the larger VTZ-F12 basis set. This changed the formation energy with respect to free reactants by −0.35 kcal/mol for the reactant adduct, and by 0.04 kcal/mol for the transition state. This indicates that basis-set effects are not a major error source in the CCSD(T)-F12 calculations.[44] Using VTZ-F12 values instead of VDZ-F12 values changes the computed elementary reaction rates to $k_{diss,3} \approx 0.16\ s^{-1}$ and $k_{ox,3} \approx 570\ s^{-1}$. However, this leaves the $(CH_3)_2COO + SO_2$ reaction rate essentially unchanged, as $k_{diss,3}$ is still significantly smaller than $k_{ox,3}$. The use of hard-sphere collision rates may also overestimate the true adduct formation rate due to the neglect of steric effects, but likely by less than a factor of 2 or 3.

Another possible error source is the neglect of pressure effects. The cyclic adducts are initially formed with an excess energy corresponding to the binding enthalpy and may decompose before they are collisionally stabilized by gas molecules (mainly N_2). However, the $(CH_3)_2COOSO_2$ adduct has 36 vibrational degrees of freedom over which the excess energy can be distributed. Even the smaller H_2COOSO_2 adduct has 18 vibrational degrees of freedom. To estimate the magnitude of pressure effects, we performed bimolecular quantum Rice−Ramsberger−Kassel (QRRK) calculations[63−65] as described by Kuang,[66] with the collisional parameters given in Kurtén et al.,[67] using the rule-of-thumb estimate[68] that half of the vibrational degrees of freedom are accessible for distributing the excess energy. We obtained energy accommodation factors (fractions of the molecules that are collisionally stabilized) at 1 atm pressure of around 0.95−0.99 for the H_2COOSO_2 adduct and above 0.99 for the $(CH_3)_2COOSO_2$ adduct, with the precise value depending slightly on, for example, the assumed density and whether B3LYP enthalpies or CCSD(T)-F12-corrected enthalpies are used. The value for the $(CH_3)_2COOSO_2$ adduct may be overestimated as the CH-stretching vibrations may not be accessible for distributing the energy liberated in the C−O and S−O bond formation. As an extreme case, we calculated the energy accommodation factor for the $(CH_3)_2COOSO_2$ adduct using only nine accessible modes (this corresponds to treating the CH_3 groups as single atoms, and then taking half the number of modes), and obtained accommodation factors of around 0.75−0.8. QRRK calculations thus indicate that, though pressure effects may play a role, most of the adducts formed in the $SO_2 + CH_2OO$ and $SO_2 + (CH_3)_2COO$ reactions are collisionally stabilized before they have time to decompose, justifying our use of the steady-state approach above. However, we caution that the QRRK framework for treating pressure dependence is quite crude.

Even though basis-set or pressure effects can thus not account for the difference between experimental and computed results, we caution that other error sources may still be present in the CCSD(T)-F12 calculations, as illustrated, for example, by the moderate T1 values encountered for the Criegee intermediates [around 0.03 for free $(CH_3)_2COO$]. Furthermore, while the CCSD(T)-F12 energies are likely reliable, the use of B3LYP structures and thermal corrections may introduce errors of a few kcal/mol. Errors in the reaction rate of a few orders of magnitude might also easily be introduced by the rather crude kinetic framework of elementary transition-state theory. Alternatively, if the lifetimes of the CIs with respect to unimolecular decomposition are shorter than estimated in the calculation of Johnson et al.,[27] the bimolecular reaction rates might well be somewhat higher than reported. A third possibility is the existence of an unknown and fast reaction mechanism by which the cyclic adduct shown in Figure 9 might form OH radicals instead of SO_3.

Regardless of whether it is due to the very short lifetimes of Criegee intermediates or to a low bimolecular rate constant, it is likely that the central conclusion of Johnson et al. that the $(CH_3)_2COO + SO_2$ reaction does not play a role in the atmosphere is correct. Drozd et al. recently studied[69] the ozonolysis of 2,3-dimethyl-2-butene (containing six carbon atoms) and found that even the stabilized Criegee intermediates decompose unimolecularly within a time scale of hundreds of milliseconds. This indicates that bimolecular reactions of CIs with trace gases, such as SO_2, are improbable, though not impossible if they indeed occur at the collision rate. Larger SCIs, such as those formed from the ozonolysis of biogenic mono- or sesquiterpenes (with 9 and 15 carbon atoms, respectively), are predicted to have higher stabilization ratios,[70] and possibly longer lifetimes with respect to unimolecular decomposition. It is not yet known if this increased stabilization also corresponds to a decrease in chemical reactivity for bimolecular reactions. Nevertheless, some of these larger SCIs might have long enough lifetimes with respect to unimolecular decomposition, but still react rapidly enough with SO_2, to contribute to SO_3 formation in some conditions. This is supported by the recent study of Jiang et al.,[23] in which the reactions of various nine-carbon SCIs were predicted to have energetics similar to the $(CH_3)_2COO + SO_2$ studied here. Experimental measurements of SO_2 oxidation in the presence of mono- or sesquiterpenes at low-OH, high-O_3 conditions, together with more advanced kinetic modeling, would likely be required to assess the overall importance of this reaction type.

4. CONCLUSIONS

The reaction of peroxyradicals with SO_2 is too slow to contribute significantly to the formation of SO_3 and sulfuric acid under any realistic atmospheric conditions. Water catalysis, or electronic excitation by UV or NIR photons, is unlikely to change this qualitative conclusion. Carbonyl oxides (Criegee intermediates), on the other hand, were found to oxidize SO_2 into SO_3 very rapidly. This is in disagreement with experimental results on the system, possibly due to uncertainties in the computational results as well as in the estimates of the lifetimes of carbonyl oxides.

■ ASSOCIATED CONTENT

Supporting Information. Table of electronic energies, enthalpies, and free energies for all studied structures and table of Cartesian coordinates for all studied structures. This material is available free of charge via the Internet at http://pubs.acs.org.

■ AUTHOR INFORMATION

Corresponding Author

*E-mail: theo.kurten@helsinki.fi (T.K.), hgk@chem.ku.dk (H.G.K.).

■ ACKNOWLEDGMENT

Michael Boy is acknowledged for helpful discussions on atmospheric chemistry. We thank the Academy of Finland, the Danish Council for Independent Research—Natural Sciences, and the Marsden Fund administered by the Royal Society of New Zealand, for funding. We thank the CSC IT Centre for Science in Espoo, Finland, the Danish Centre for Scientific Computing (DCSC), and the University of Waikato High Performance Computing Facility, for computer time. S.J. is grateful for a Freia Fellowship from the Faculty of Science, University of Copenhagen.

■ REFERENCES

(1) Solomon, S.; Qin, D.; Manning, M.; Chen, Z.; Marquis, M.; Averyt, K. B.; Tignor, M.; Miller, H. L., Eds. *Contribution of Working Group I to the Fourth Assessment Report of the Intergovernmental Panel on Climate Change* ; Cambridge University Press: Cambridge, U.K., 2007.

(2) Kulmala, M.; Vehkamäki, H.; Petäjä, T.; Dal Maso, M.; Lauri, A.; Kerminen, V.-M.; Birmili, W.; McMurry, P. H. *J. Aerosol Sci.* **2004**, *35*, 143.

(3) Sipilä, M.; Berndt, T.; Petäjä, T.; Brus, D.; Vanhanen, J.; Stratmann, F.; Patokoski, J.; Mauldin, R. L., III; Hyvärinen, A.-P.; Lihavainen, H.; Kulmala, M. *Science* **2010**, *327*, 1243.

(4) Nadykto, A. B.; Yu, F. *Chem. Phys. Lett.* **2007**, *435*, 14.

(5) Kurtén, T.; Loukonen, V.; Vehkamäki, H.; Kulmala, M. *Atmos. Chem. Phys.* **2008**, *8*, 4095.

(6) Petäjä, T.; Sipilä, M.; Paasonen, P.; Nieminen, T.; Kurtén, T.; Berndt, T.; Stratmann, F.; Vehkamäki, H.; Kulmala, M. *Phys. Rev. Lett.* **2011**in press.

(7) Wayne, R. P. *Chemistry of Atmospheres*, 3rd ed.; Oxford University Press: Oxford, U.K., 2000.

(8) Atkinson, R.; Baulch, D. L.; Cox, R. A.; Crowley, J. N.; Hampson, R. F.; Hynes, R. G.; Jenkin, M. E.; Rossi, M. J.; Troe, J. *Atmos. Chem. Phys.* **2004**, *4*, 1461.

(9) DeMore, W. B.; Sander, S. P.; Golden, G. M.; Hampson, R. F.; Kurylo, M. J.; Howard, C. J.; Ravishankara, A. R.; Kolb, C. E; Molina, M. J. *Chemical kinetics and photochemical data for use in stratospheric modelling*; Evaluation number 12; JPL Publication 97-4, 1-266; Jet Propulsion Laboratory: Pasadena, CA, 1997.

(10) Kurtén, T.; Lane, J. R.; Jørgensen, S.; Kjaergaard, H. G. *Phys. Chem. Chem. Phys.* **2010**, *12*, 12833.

(11) Sorokin, A. *Atmos. Chem. Phys.* **2010**, *10*, 3141.

(12) Personal communication with M. Boy, based on results from EUCAARI project field campaign in spring 2007.

(13) Wang, B.; Hou, H. *Chem. Phys. Lett.* **2005**, *410*, 235.

(14) Graham, R. A.; Winer, A. M.; Atkinson, R.; Pitts, J. N., Jr. *J. Phys. Chem.* **1979**, *83*, 1563.

(15) Kan, C. S.; McQuiff, R. D.; Whitbeck, M. R.; Calvert, J. G. *Int. J. Chem. Kinet.* **1979**, *11*, 921.

(16) Sanhueza, E.; Simonaitis, R.; Hecklen, J. *Int. J. Chem. Kinet.* **1979**, *11*, 907.

(17) Sander, S. P.; Watson, R. T. *Chem. Phys. Lett.* **1981**, *77*, 473.

(18) Kan, C. S.; Calvert, J. G.; Shaw, J. H. *J. Phys. Chem.* **1981**, *85*, 1126.

(19) Cocks, A. T.; Fernando, R. P.; Fletcher, I. S. *Atmos. Environ.* **1986**, *20*, 2359.

(20) Criegee, R. *Chem. Ber.* **1944**, *77*, 722.

(21) Taatjes, C. A.; Meloni, G.; Selby, T. M.; Trevitt, A. J.; Osborn, D. L.; Percival, C. J.; Shallcross, D. E. *J. Am. Chem. Soc.* **2008**, *130*, 11883.

(22) Calvert, J. G.; Lazrus, A.; Kok, G. L.; Heikes, B. G.; Walega, J. G.; Lind, J.; Cantrell, C. A. *Nature* **1985**, *317*, 27.

(23) Hatakeyama, S.; Kobayashi, H.; Lin, Z. Y.; Tagaki, H.; Akimoto, H. *J. Phys. Chem.* **1986**, *90*, 4131.

(24) Johnson, D.; Lewin, A. G.; Marston, G. *J. Phys. Chem. A* **2001**, *105*, 2933.

(25) Kroll, J. H.; Sahay, S. R.; Anderson, J. G.; Demerjian, K. L.; Donahue, N. M. *J. Phys. Chem. A* **2001**, *105*, 4446.

(26) Aplincourt, P.; Ruiz-López, M. F. *J. Am. Chem. Soc.* **2000**, *122*, 8990.

(27) Jiang, L.; Xu, Y.; Ding, A. *J. Phys. Chem. A* **2010**, *114*, 12452.

(28) Wheeler, S. E.; Ess, D. H.; Houk, K. N. *J. Phys. Chem. A* **2008**, *112*, 1798.

(29) Becke, A. D. *J. Chem. Phys.* **1993**, *98*, 5648.

(30) Lee, C.; Yang, W.; Parr, R. G. *Phys. Rev. B* **1998**, *37*, 785.

(31) Dunning, T. H., Jr.; Peterson, K. A.; Wilson, A. K. *J. Chem. Phys.* **2001**, *114*, 9244.

(32) Wilson, A.; Dunning, T. H., Jr. *J. Phys. Chem. A* **2004**, *108*, 3129.

(33) Adler, G.; Knizia, T. B.; Werner, H.-J. *J. Chem. Phys.* **2007**, *127*, 221106.

(34) Peterson, K. A.; Adler, T. B.; Werner, H.-J. *J. Chem. Phys.* **2008**, *128*, 084102.

(35) Kutzelnigg, W.; Klopper, W. *J. Chem. Phys.* **1991**, *94*, 1985.

(36) Tew, D. P.; Klopper, W.; Neiss, C.; Hättig, C. *Phys. Chem. Chem. Phys.* **2007**, *9*, 1921.

(37) Knizia, G.; Adler, T. B.; Werner, H.-J. *J. Chem. Phys.* **2009**, *130*, 054104.

(38) Manby, F. R. *J. Chem. Phys.* **2003**, *119*, 4607.

(39) Werner, H.-J.; Adler, T. B.; Manby, F. R. *J. Chem. Phys.* **2007**, *126*, 164102.

(40) Weigend, F.; Köhn, A.; Hättig, C. *J. Chem. Phys.* **2002**, *116*, 3175.

(41) Weigend, F. *Phys. Chem. Chem. Phys.* **2002**, *4*, 4285.

(42) Yousaf, K. E.; Peterson, K. A. *J. Chem. Phys.* **2008**, *129*, 184108.

(43) Knizia, G.; Adler, T. B.; Werner, H.-J. *J. Chem. Phys.* **2009**, *130*, 054104.

(44) Lane, J. R.; Kjaergaard, H. G. *J. Chem. Phys.* **2009**, *131*, 034307.

(45) Cremer, D.; Kraka, E.; Szalay, P. G. *Chem. Phys. Lett.* **1998**, *292*, 97.

(46) Schaftenaar, G.; Noordik, J. H. *J. Comput.-Aided Mol. Des.* **2000**, *14*, 123.

(47) Schuchardt, K. L.; Didier, B. T.; Elsethagen, T.; Sun, L.; Gurumoorthi, V.; Chase, J.; Li, J.; Windus, T. L. *J. Chem. Inf. Model* **2007**, *47*, 1045.

(48) Frisch, M. J.; Trucks, G. W.; Schlegel, H. B.; Scuseria, G. E.; Robb, M. A.; Cheeseman, J. R.; Scalmani, G.; Barone, V.; Mennucci, B.; Petersson, G. A.; Nakatsuji, H.; Caricato, M.; Li, X.; Hratchian, H. P.; Izmaylov, A. F.; Bloino, J.; Zheng, G.; Sonnenberg, J. L.; Hada, M.; Ehara, M.; Toyota, K.; Fukuda, R.; Hasegawa, J.; Ishida, M.; Nakajima, T.; Honda, Y.; Kitao, O.; Nakai, H.; Vreven, T.; Montgomery, J. A., Jr.; Peralta, J. E.; Ogliaro, F.; Bearpark, M.; Heyd, J. J.; Brothers, E.; Kudin, K. N.; Staroverov, V. N.; Kobayashi, R.; Normand, J.; Raghavachari, K.; Rendell, A.; Burant, J. C.; Iyengar, S. S.; Tomasi, J.; Cossi, M.; Rega, N.; Millam, N. J.; Klene, M.; Knox, J. E.; Cross, J. B.; Bakken, V.; Adamo, C.; Jaramillo, J.; Gomperts, R.; Stratmann, R. E.; Yazyev, O.; Austin, A. J.; Cammi, R.; Pomelli, C.; Ochterski, J. W.; Martin, R. L.; Morokuma, K.; Zakrzewski, V. G.; Voth, G. A.; Salvador, P.; Dannenberg, J. J.; Dapprich, S.; Daniels, A. D.; Farkas, Ö.; Foresman, J. B.; Ortiz, J. V.; Cioslowski, J.; Fox, D. J. *Gaussian 09*, revision A.1; Gaussian, Inc.: Wallingford, CT, 2009.

(49) Werner, H.-J.; Knowles, P. J.; Manby, F. R.; Schültz, M.; Celani, P.; Knizia, G.; Korona, T.; Lindh, R.; Mitrushenkov, A.; Rauhut, G.; Adler, T. B.; Amos, R. D.; Bernhardsson, A.; Berning, A.; Cooper, D. L.; Deegan, M. J. O.; Dobbyn, A. J.; Eckert, F.; Goll, C.; Hampel, C.; Hesselmann, A.; Hetzer, G.; Hrenar, T.; Jansen, G.; Köppl, C.; Liu, Y.; Lloyd, A. W.; Mata, R. A.; May, A. J.; McNicholas, S. J.; Meyer, W.; Mura, M. E.; Nicklass, A.; Palmieri, P.; Pflüger, K.; Pitzer, R.; Reiher, T.; Shiozaki, H.; Stoll, H.; Stone, A. J.; Tarroni, R.; Thorsteinsson, T.; Wang, M.; Wolf, A. *MOLPRO*, version 2010.1; 2010. See http://www.molpro.net.

(50) Ehn, M.; Junninen, H.; Petäjä, T.; Kurtén, T.; Kerminen, V.-M.; Schobesberger, S.; Manninen, H. E.; Ortega, I. K.; Vehkamäki, H.; Kulmala, M.; Worsnop, D. R. *Atmos. Chem. Phys.* **2010**, *10*, 8513.

(51) Jørgensen, S.; Kjaergaard, H. G. *J. Phys. Chem. A* **2010**, *114*, 4857.

(52) Luo, Y.; Maeda, S.; Ohno, K. *Chem. Phys. Lett.* **2009**, *469*, 57.
(53) Vohringer-Martinez, E.; Hansmann, B.; Hernandez, H.; Francisco, J. S.; Troe, J.; Abel, B. *Science* **2007**, *315*, 497.
(54) Kurtén, T.; Berndt, T.; Stratmann, F. *Atmos. Chem. Phys.* **2009**, *9*, 3357.
(55) Clark, J.; English, A. M.; Hansen, J. C.; Francisco, J. S. *J. Phys. Chem. A* **2008**, *112*, 1587.
(56) Buszek, R. J.; Sinha, A.; Francisco, J. S. *J. Am. Chem. Soc.* **2011**, *133*, 2013.
(57) Wallington, T. J.; Dagaut, P.; Kurylo, M. J. *Chem. Rev.* **1992**, *92*, 667.
(58) Jafri, J. A.; Phillips, D. H. *J. Am. Chem. Soc.* **1990**, *112*, 2586.
(59) Hunziker, H. E.; Wendt, H. R. *J. Chem. Phys.* **1976**, *64*, 3488.
(60) Sharp, E. N. Observation of the A ~ X Electronic Transition in Peroxy Radicals Using Cavity Ringdown Spectroscopy. Ph.D. Thesis, The Ohio State University, Columbus, OH, 2008. Available online at http://drc.ohiolink.edu/handle/2374.OX/6578.
(61) Frost, G. J.; Ellison, G. B.; Vaida, V. *J. Phys. Chem. A* **1999**, *103*, 10169.
(62) Melnik, D.; Chhantyal-Pun, R.; Miller, T. A. *J. Phys. Chem. A* **2010**, *114*, 11583.
(63) Dean, A. M. *J. Phys. Chem.* **1985**, *89*, 4600.
(64) Rice, O. K.; Ramsperger, H. C. *J. Am. Chem. Soc.* **1927**, *49*, 1617.
(65) Kassel, L. S. *J. Phys. Chem.* **1928**, *32*, 1065.
(66) Kuang, C. Atmospheric nucleation: Measurements, mechanisms, and dynamics. Ph.D. Thesis, University of Minnesota, Minneapolis, MN, 2009.
(67) Kurtén, T.; Kuang, C.; Gómez, P.; McMurry, P. H.; Vehkamäki, H.; Ortega, I. K.; Noppel, M.; Kulmala, M. *J. Chem. Phys.* **2010**, *132*, 024304.
(68) Laidler, K. J. *Chemical Kinetics*; Harper: New York, 1987.
(69) Drozd, G. T.; Kroll, J.; Donahue, N. M. *J. Phys. Chem. A* **2011**, *115*, 161.
(70) Chuong, D.; Zhang, J. Y.; Donahue, N. M. *J. Am. Chem. Soc.* **2004**, *126*, 12363.